Optical Properties of Drug Metabolites in Latent Fingermarks

Yao Shen[1,*] **and Qing Ai**[2]

[1]School of Forensic Science, People's Public Security University of China, Beijing 100038, China
[2]Department of Physics, Applied Optics Beijing Area Major Laboratory, Beijing Normal University, Beijing 100875, China
*shenyaophysics@hotmail.com

ABSTRACT

Drug metabolites usually have structures of split-ring resonators (SRRs), which might lead to negative permittivity and permeability in electromagnetic field. As a result, in the UV-vis region, the latent fingermarks images of drug addicts and non drug users are inverse. The optical properties of latent fingermarks are quite different between drug addicts and non-drug users. This is a technic superiority for crime scene investigation to distinguish them. In this paper, we calculate the permittivity and permeability of drug metabolites using tight-binding model. The latent fingermarks of smokers and non-smokers are given as an example.

In 1968, negative index material (NIM) was first introduced by Veselago.[1] NIM can have negative permittivity and permeability simultaneously. Pendry *et al.*[2–6] gave a deep discussion and pointed out that a configuration which was called split-ring resonator (SRR)[3] could put negative refraction into practice, apart from some particular configurations with non-trivial symmetry breaking.[7] From then on, negative refraction became a focus in scientific research, for example NIM can be used to fabricate perfect lenses to enhance local field and detection sensitivity.[8–12] Two years later, Shelby *et al.*[13] realized NIM experimentally. Metamaterial, made up of SRRs or molecules which consist of SRRs, e.g. extended metal atom chains, becomes a new branch of study.[14–38] Many new directions are developed, such as electromagnetic cloaking,[39–44] toroidal moment,[45] liquid crystal magnetic control,[46] etc. On the other hand, in forensic science, on highly reflective surface, the latent fingermarks are difficult to be observed. The traditional method of visualizing the invisible fingermarks is using fluorescent tag. In Boddis and Russell's paper,[49] they made use of antibody-magnetic particle conjugates to visualize them. During this procedure, they find the latent fingermarks of smokers and non-smokers are quite different. As a result, the latent fingermarks of these two kinds of donors are observed to be inverse and thus they can be used to identify the smokers. The research of distinguishing drug users by metabolites becomes a new focus in forensic science field.[47,48] In this paper, we first introduce negative refraction phenomenon to forensic science. We point out that when we put those latent fingermarks of drug addicts and non-drug users in the light field, they can also be identified. Furthermore, our method is physical and non-damaged, because the latent fingermarks will not be destroyed. More importantly, due to quantum effect, a small volume of molecules could sufficiently respond negatively to the applied electromagnetic fields.[50] We give the theoretical derivation and calculation of this phenomenon. Our result is not only suitable for smokers but also for drug addicts. In other words, except for cotinine, the metabolite of nicotine, benzoylecgonine and morphine can also be detected using our method.

This paper is organized as following: In section II, we give the theoretical derivation of the permittivity and permeability of cotinine on the basis of tight-binding model. And we discuss the numerical results of permittivity and permeability. Finally, the main results are concluded and future work is discussed in the discussion section.

Results

Tight-binding Approximation and Hückel Model

Many molecules of drug metabolites have a broken ring configuration, i.e. SRRs. This structure gives them special optical properties. Without loss of generality, we calculate cotinine, i.e. the metabolite of nicotine, as an example.

Figure 1(a) demonstrate the structure of cotinine molecule. The main part of cotinine is the hexagon part which is called pyridine (see Figure 1 (b)). In this part, one carbon atom of the ring is substituted with one nitrogen atom, and for the sake of simplicity the remaining part of cotinine molecule is simplified into a methyl in the same plane. This simplification is reasonable because the main contribution to the optical property comes from the π electrons of conjugate part of cotinine molecule (single-nitrogen-substituted heterocyclic annulene[51]).
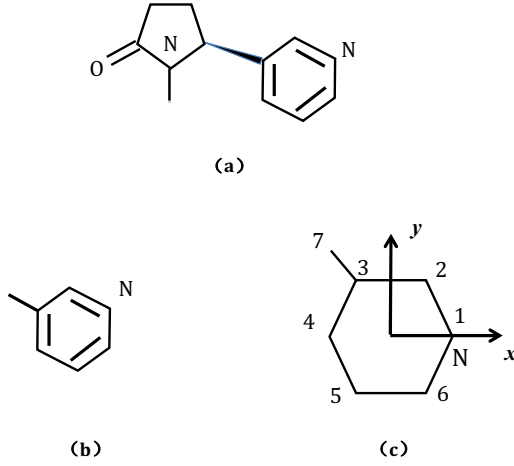
Figure 1. (a) The chemical structure of cotinine molecule ($C_{10}H_{12}N_2O$). Cotinine has two rings, one is pyridyl, and the other is pyrrolidin. (b) The simplified model. The molecule is simplified into a pyridyl and a methyl. (c) The spatial distribution of atoms in the simplified model. The origin is set at the center of the hexagon. Seven sites are labeled sequentially. Site 1 is a nitrogen atom and others are carbon atoms.

π electrons of the pyridyl interact with the electromagnetic fields which results in special optical properties of cotinine. The structure consists of one pyridyl and one methyl with sites labeled as Figure 1(c). The quantum dynamics of π electrons around these seven sites are described by the Hückel model as[52]

$$\mathscr{H} = \sum_{j=1}^{6} \alpha_j |j\rangle \langle j| + \alpha_C |7\rangle \langle 7| + \sum_{j=1}^{6} \beta_{j,j+1} (|j\rangle \langle j+1| + |j+1\rangle \langle j|) + \beta_{CC} (|3\rangle \langle 7| + |7\rangle \langle 3|), \tag{1}$$

where j is the site label, $|j\rangle$ denotes the state with a π electron at site j, α_j is the site energy, the coupling strength between jth and $(j+1)$th sites is given by the resonant integral $\beta_{j,j+1}$. Here, when $j = 6$, the adjacent site is not site 7 but site 1. The nitrogen atom is located at site 1 (see Figure 1(c)). In this configuration, the site energies and coupling constants are explicitly given as

$$\alpha_j = \begin{cases} \alpha_C, \text{ for } j \neq 1, \\ \alpha_N, \text{ for } j = 1, \end{cases} \tag{2}$$

$$\beta_{j,j+1} = \begin{cases} \beta_{CC}, \text{ for } j \neq 1,6, \\ \beta_{CN}, \text{ for } j = 1,6. \end{cases} \tag{3}$$

By diagonalization, the Hückel Hamiltonian (1) can be reexpressed as

$$\mathscr{H} = \sum_{k=1}^{7} \varepsilon_k |\psi_k\rangle \langle \psi_k|, \tag{4}$$

where

$$|\psi_k\rangle = \sum_{j=1}^{7} C_{ki} |j\rangle$$

is kth single-electron molecular orbital, ε_k is energy level.

In order to obtain $|\psi_k\rangle$ and ε_k , we use the perturbation theory in quantum mechanics. We assume that the unperturbed system is a benzene and an isolated methyl, i.e.

$$\begin{aligned} H_0 &= \sum_{j=1}^{7} \alpha |j\rangle \langle j| + \sum_{j=1}^{6} \beta_{j,j+1} (|j\rangle \langle j+1| + |j+1\rangle \langle j|) \\ &= \sum_{k=1}^{6} \varepsilon_k^{(0)} |k\rangle \langle k| + \alpha |7\rangle \langle 7|, \end{aligned} \tag{5}$$

where

$$|k\rangle = \frac{1}{\sqrt{6}} \sum_{j=1}^{6} e^{-ikj} |j\rangle, \tag{6}$$

$$\varepsilon_k^{(0)} = \alpha + 2\beta \cos k \tag{7}$$

with momentum $k = m\pi/3$ and $m = -3, -2, -1, 0, 1, 2$. For simplicity, we use $\alpha = \alpha_{CC}$ and $\beta = \beta_{CC}$. The isolated methyl contributes an isolated eigen state $|7\rangle$ with eigen energy α. Then, the perturbation originates from

$$H' = \mathscr{H} - H_0 = \Delta\alpha \left(a_1^\dagger a_1\right) + \Delta\beta \left(a_1^\dagger a_2 + a_2^\dagger a_1 + a_1^\dagger a_6 + a_6^\dagger a_1\right) + \beta \left(a_3^\dagger a_7 + a_7^\dagger a_3\right), \tag{8}$$

where $a_j^\dagger |0\rangle = |j\rangle$ and $a_j |j\rangle = |0\rangle$ with $|0\rangle$ being the vacuum state, $\Delta\alpha = \alpha_N - \alpha_C$ and $\Delta\beta = \beta_{CN} - \beta_{CC}$. $a_j^\dagger$ is the creation operator on jth site and a_j is the annihilation operator. Benzene has four energy levels $\varepsilon_1, \varepsilon_2, \varepsilon_3, \varepsilon_4$, which are labeled sequencially from the lowest eigen energy. Both the degeneracies of ε_2 and ε_3 are two, while ε_1 and ε_4 are non-degenerate. Because one nitrogen atom substitutes for one carbon atom in the pyridyl, the degeneracy is lifted. As a consequence, the simplified cotinine molecule has seven energy levels (see Figure 2), and all of them are non-degenerate with the methyl giving the additional ε_0. For the sake of simplicity, we further assume $\alpha = 0$.

According to the perturbation theory, the energy spectrum of the simplified cotinine molecule reads

$$\varepsilon_1^{(1)} = \frac{1}{6}\Delta\alpha + \frac{2}{3}\Delta\beta + \frac{2\beta}{\sqrt{6}}, \tag{9}$$

$$\varepsilon_{21}^{(1)} = \frac{1}{6}\left[\Delta\alpha - 2\Delta\beta + 2\sqrt{6}\beta - \sqrt{\Delta\alpha^2 + 2\Delta\alpha\left(\Delta\beta + 2\sqrt{6}\beta\right) + \left(\Delta\beta^2 + 4\sqrt{6}\Delta\beta\beta + 24\beta^2\right)}\right],$$

$$\varepsilon_{22}^{(1)} = \frac{1}{6}\left[\Delta\alpha - 2\Delta\beta + 2\sqrt{6}\beta + \sqrt{\Delta\alpha^2 + 2\Delta\alpha\left(\Delta\beta + 2\sqrt{6}\beta\right) + \left(\Delta\beta^2 + 4\sqrt{6}\Delta\beta\beta + 24\beta^2\right)}\right],$$

$$\varepsilon_{31}^{(1)} = \frac{1}{6}\left[\Delta\alpha + 2\Delta\beta - 2\sqrt{6}\beta - \sqrt{\Delta\alpha^2 - 2\Delta\alpha\left(\Delta\beta + 2\sqrt{6}\beta\right) + \left(\Delta\beta^2 + 4\sqrt{6}\Delta\beta\beta + 24\beta^2\right)}\right],$$

$$\varepsilon_{32}^{(1)} = \frac{1}{6}\left[\Delta\alpha + 2\Delta\beta - 2\sqrt{6}\beta + \sqrt{\Delta\alpha^2 + 2\Delta\alpha\left(\Delta\beta + 2\sqrt{6}\beta\right) + \left(\Delta\beta^2 + 4\sqrt{6}\Delta\beta\beta + 24\beta^2\right)}\right],$$

$$\varepsilon_4^{(1)} = \frac{1}{6}\Delta\alpha - \frac{2}{3}\Delta\beta - \frac{2\beta}{\sqrt{6}},$$

$$\varepsilon_{|7\rangle}^{(1)} = 0.$$

Following the degenerate perturbation theory, we can obtain the wave function to the first order. Since their explicit expressions are very complicated, we do not list them here.

The cotinine molecule has seven non-interacting π-electrons which fill in seven energy levels. The energy levels are illustrated in Figure 2. On account of the spin degree (see Figure 3), the ground state can be expressed in the second-quantization form as

$$|\Psi_0\rangle = a_{1\uparrow}^\dagger a_{1\downarrow}^\dagger a_{2\uparrow}^\dagger a_{2\downarrow}^\dagger a_{3\uparrow}^\dagger a_{3\downarrow}^\dagger a_{4\uparrow}^\dagger |0\rangle, \tag{10}$$

and we use E_0 to represent the ground-state energy of the whole cotinine system, i.e.

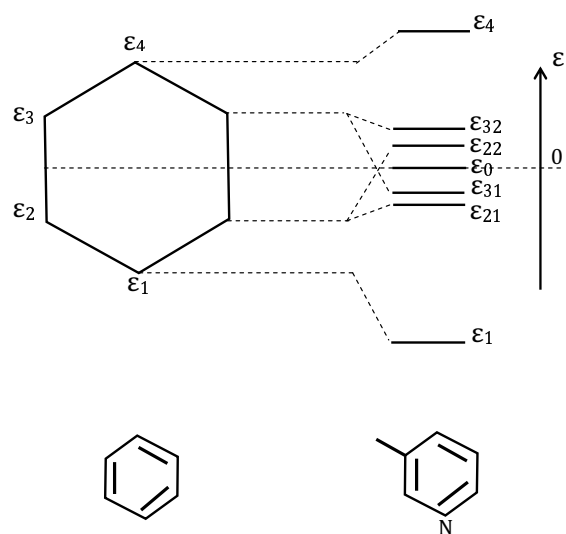$$E_0 = 2(\varepsilon_1 + \varepsilon_2 + \varepsilon_3) + \varepsilon_4, \tag{11}$$

where $a_{k\sigma}^\dagger$ is the creation operator of the orbital k with spin σ ($\sigma = \uparrow, \downarrow$).

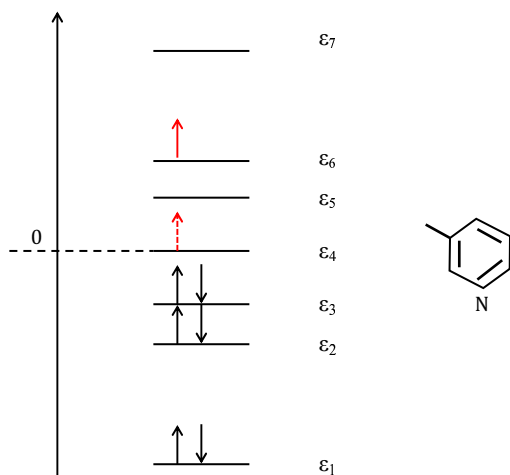The system has twenty seven single-excitation states, for example, the 2th and 11th excitation states are

$$|\Psi_2\rangle = a_{1\uparrow}^\dagger a_{1\downarrow}^\dagger a_{2\uparrow}^\dagger a_{2\downarrow}^\dagger a_{3\uparrow}^\dagger a_{3\downarrow}^\dagger a_{6\uparrow}^\dagger |0\rangle,$$
$$|\Psi_{11}\rangle = a_{1\uparrow}^\dagger a_{1\downarrow}^\dagger a_{2\uparrow}^\dagger a_{2\downarrow}^\dagger a_{3\uparrow}^\dagger a_{7\downarrow}^\dagger a_{4\uparrow}^\dagger |0\rangle,$$

with corresponding eigen energies

$$E_2 = 2(\varepsilon_1 + \varepsilon_2 + \varepsilon_3) + \varepsilon_6,$$
$$E_{11} = 2(\varepsilon_1 + \varepsilon_2) + \varepsilon_3 + \varepsilon_4 + \varepsilon_7,$$

Figure 2. The energy spectra of (left) benzene and (right) simplified cotinine molecule.

Figure 3. The single-electron excitation of cotinine molecule (red solid up-arrow) from the ground state (red dashed up-arrow).

respectively. In the first case, the electron with energy ε_4 and spin up is excited to energy level ε_6. In the second case, the electron with energy ε_3 and spin down is excited to energy level ε_7. Here the flip of electronic spin is not taken into consideration. To sum up, the single-excitation states read

$$|\Psi_n\rangle = \left|\Psi_{p\sigma}^{q\sigma}\right\rangle = a_{q\sigma}^{\dagger} a_{p\sigma} |\Psi_0\rangle, \tag{12}$$

where $p = 1,2,3,4$, $q = 4,5,6,7$ and $\sigma = \uparrow, \downarrow$, an the eigen energies are

$$E_n = E_0 + \varepsilon_q - \varepsilon_p. \tag{13}$$

In the subspaces spanned by the ground state and single-excitation states, the Hamiltonian without electro-magnetic field reads

$$\mathcal{H} = \sum_{n=0}^{27} E_n |\Psi_n\rangle \langle \Psi_n|. \tag{14}$$

Perturbation Theory in Electromagnetic Field

When there is a time-dependent electromagnetic field applied on the molecule, based on the dipole approximation, the total Hamiltonian including the interaction between the molecule and the electromagnetic field can be written as

$$
\begin{aligned}
H &= \mathcal{H} - \vec{\mu} \cdot \vec{E}(\vec{r},t) - \vec{m} \cdot \vec{B}(\vec{r},t) \\
&\simeq \mathcal{H} - \vec{\mu} \cdot \vec{E}_0 \cos(\vec{k} \cdot \vec{r} - \omega t) - \vec{m} \cdot \vec{B}_0 \cos(\vec{k} \cdot \vec{r} - \omega t),
\end{aligned}
\tag{15}
$$

where $\mathcal{H}$ is the Hamiltonian without electromagnetic field, $\vec{\mu}$ and $\vec{m}$ denote the electric and magnetic dipole moments respectively. By assuming the spatial scale of the molecule is much smaller than the wave length of the field $\vec{k} \cdot \vec{r} \simeq 0$ (the coordinate is chosen as Figure 1(c)), we have

$$H \simeq \mathcal{H} - \vec{\mu} \cdot \vec{E}_0 \cos(\omega t) - \vec{m} \cdot \vec{B}_0 \cos(\omega t). \tag{16}$$

By a unitary transformation

$$U^{\dagger} = \exp\left(-i\omega |\Psi_0\rangle \langle \Psi_0| t\right), \tag{17}$$

the Hamiltonian becomes time-independent

$$
\begin{aligned}
H' &= U^{\dagger} H U - i U^{\dagger} \dot{U} \\
&\simeq \sum_{n=1}^{27} E_n |\Psi_n\rangle \langle \Psi_n| + (E_0 + \omega) |\Psi_0\rangle \langle \Psi_0| + H'',
\end{aligned}
\tag{18}
$$

where

$$
\begin{aligned}
H'' &= -\frac{1}{2} \sum_{n=1}^{27} \left(\vec{\mu}_{n0} \cdot \vec{E}_0 |\Psi_n\rangle \langle \Psi_0| + \vec{\mu}_{0n} \cdot \vec{E}_0 |\Psi_0\rangle \langle \Psi_n| \right) \\
&\quad -\frac{1}{2} \sum_{n=1}^{27} \left(\vec{m}_{n0} \cdot \vec{B}_0 |\Psi_n\rangle \langle \Psi_0| + \vec{m}_{0n} \cdot \vec{B}_0 |\Psi_0\rangle \langle \Psi_n| \right),
\end{aligned}
\tag{19}
$$

$$\vec{\mu}_{nn'} = \langle \Psi_n | \vec{\mu} | \Psi_{n'} \rangle, \tag{20}$$

$$\vec{m}_{nn'} = \langle \Psi_n | \vec{m} | \Psi_{n'} \rangle. \tag{21}$$

In other words, we change the system from the static frame into a rotating frame. In the rotating frame, the state and operator become $|\Psi'\rangle = U^{\dagger} |\Psi\rangle$, and $A' = U^{\dagger} A U$, respectively. Moreover, due to the interaction with electromagnetic field, the molecular ground state becomes

$$\left|\Psi_0'\right\rangle = U^{\dagger} |\Psi_0\rangle = |\Psi_0\rangle + \sum_{n=1}^{27} \frac{\langle \Psi_n | H'' | \Psi_0 \rangle}{E_0 + \omega - E_n} |\Psi_n\rangle, \tag{22}$$

Permittivity

The electric dipole moment in the rotating frame reads

$$\vec{\mu}' = U^\dagger \vec{\mu} U = \sum_{n=1}^{27} \left(\vec{\mu}_{n0} e^{i\omega t} |\Psi_n\rangle \langle \Psi_0| + \vec{\mu}_{0n} e^{-i\omega t} |\Psi_0\rangle \langle \Psi_n| \right). \tag{23}$$

For the ground state, the expectation value for the dipole operator in the rotating frame is

$$\left\langle \Psi_0' \middle| \vec{\mu}' \middle| \Psi_0' \right\rangle = -\text{Re} \sum_{n=1}^{27} \frac{\vec{\mu}_{n0} \cdot \vec{E}_0}{E_0 + \omega - E_n} \vec{\mu}_{0n} e^{-i\omega t}. \tag{24}$$

In the electromagnetic field, the electric displacement field in a volume V with N identical molecules

$$
\begin{aligned}
\vec{D} &= \varepsilon \vec{E}_0 \\
&= \varepsilon_0 \varepsilon_r \vec{E}_0 \\
&= \varepsilon_0 \vec{E}_0 + \frac{\vec{P}}{V}
\end{aligned}
\tag{25}
$$

reads

$$\vec{D} = \varepsilon_0 \vec{E}_0 - \sum_{s=1}^{N} \sum_{n=1}^{27} \frac{\left[\vec{\mu}_{n0}(s) \cdot \vec{E}_0 \right] \vec{\mu}_{0n}(s)}{V(E_0 + \omega - E_n)}. \tag{26}$$

Thus, the total permittivity in different direction is

$$\varepsilon_{ij} = \varepsilon_0 \delta_{ij} - \sum_{s=1}^{N} \sum_{n=1}^{27} \frac{\mu_{0n}^{(i)}(s) \mu_{n0}^{(j)}(s)}{(E_0 + \omega - E_n) V}, \text{ for } i,j = x,y,z \tag{27}$$

The relative dielectric constant of the system, i.e. the permittivity, gives

$$\varepsilon_{ij}^r \equiv \delta_{ij} - \sum_{s=1}^{N} \sum_{n=1}^{27} \frac{\vec{\mu}_{0n}(s) \cdot \hat{e}_i \vec{\mu}_{n0}(s) \cdot \hat{e}_j}{\varepsilon_0 V (E_0 + \omega - E_n)}, \text{ for } i,j = x,y,z, \tag{28}$$

where $\hat{e}_i$ is the unit vector of the lab coordinate system.

If we choose the symmetric center of benzene as the origin of coordinate (see Figure 1(c)), the electric dipole moment reads

$$\vec{\mu} = -\sum_{j=1}^{7} e \vec{r}_j, \tag{29}$$

where $\vec{r}_j$ is the vector of jth electron and $-e$ is the electric charge of electrons. Because $\vec{r}_j$'s are single-electron operators, the matrix elements of electric dipole operators are given by

$$\vec{\mu}_{0n} = \langle \Psi_0 | \vec{\mu} | \Psi_n \rangle \quad = \quad -e \langle \Psi_0 | \vec{r} | \Psi_n \rangle = -e \left\langle \psi_p \middle| \vec{r} \middle| \psi_q \right\rangle = -e \vec{r}_{pq}, \tag{30}$$

where $\vec{r}_{pq}$ is the overlap of $\vec{r}$ between two single-electron wave functions, i.e.

$$\left\langle \psi_p \middle| \vec{r} \middle| \psi_q \right\rangle = \sum_{j=1}^{7} C_{pj}^* C_{qj} \vec{r}_j. \tag{31}$$

Permeability

To account for the magnetic response of cotinine molecule, we start from the Heisenberg equations of motion,

$$
\begin{aligned}
p^x &= m_e \dot{r}^x = i m_e \left[\mathcal{H}, r^x \right], \tag{32} \\
p^y &= m_e \dot{r}^y = i m_e \left[\mathcal{H}, r^y \right], \tag{33}
\end{aligned}
$$

where we assume $\hbar = 1$ and m_e is the mass of electrons of cotinine molecule.

The magnetic dipole moment is related to the angular momentum of the system. The angular momentum operators read

$$L_x = r^y p^z - r^z p^y = 0, \tag{34}$$
$$L_y = r^z p^x - r^x p^z = 0, \tag{35}$$
$$L_z = r^x p^y - r^y p^x$$
$$= \frac{1}{2}\left(r^x p^y + p^y r^x - r^y p^x - p^x r^y\right)$$
$$= i m_e \left(r^x \mathcal{H} r^y - r^y \mathcal{H} r^x\right). \tag{36}$$

Obviously, only the response in z direction is present as all atoms in the cotinine molecule are restricted in the xy plane (see Figure 1(c)). Therefore, the magnetic dipole moment is

$$\vec{m} = \frac{-e}{2m_e}\vec{L}$$
$$= \frac{-e}{2m_e}L_z \hat{e}_z$$
$$= \frac{-ie}{2}\left(r^x \mathcal{H} r^y - r^y \mathcal{H} r^x\right)\hat{e}_z$$
$$= \frac{-ie}{2}\sum_{k,k'}\sum_n E_n \left(r_{kn}^x r_{nk'}^y - r_{kn}^y r_{nk'}^x\right)|\Psi_k\rangle\langle\Psi_{k'}|\hat{e}_z, \tag{37}$$

where

$$r_{kk'}^\alpha = \langle\psi_k| r^\alpha |\psi_{k'}\rangle. \tag{38}$$

Similar to the electric response, the expectation value for the magnetic dipole operator in the rotating frame is

$$\left\langle\Psi_0'\left|\vec{m}'\right|\Psi_0'\right\rangle = -\mathrm{Re}\sum_{n=1}^{27}\frac{\vec{m}_{n0}\cdot\vec{B}_0}{E_0+\omega-E_n}\vec{m}_{0n}e^{-i\omega t}. \tag{39}$$

The magnetic induction in a volume V with N identical molecules

$$\vec{B} = \mu\vec{H}_0$$
$$= \mu_0\mu_r\vec{H}_0$$
$$= \mu_0\vec{H}_0 + \mu_0\frac{\vec{M}}{V} \tag{40}$$

is explicitly given by

$$\vec{B} = \mu_0\vec{H}_0 - \sum_{s=1}^N\sum_{n=1}^{27}\frac{\mu_0\vec{m}_{n0}(s)\cdot\vec{B}_0}{V(E_0+\omega-E_n)}\vec{m}_{0n}(s). \tag{41}$$

Notice that μ is the permeability of medium, different from the electric dipole moment $\vec{\mu}$ above. And $\vec{H}_0$ is magnetic field intensity, not the Hamiltonian without electromagnetic field H_0.

The relative permeability of cotinine system is simplified as

$$\mu_{ij}^r \equiv \delta_{ij} - \mu_0\sum_{s=1}^N\sum_{n=1}^{27}\frac{\vec{m}_{0n}(s)\cdot\hat{e}_i\vec{m}_{n0}(s)\cdot\hat{e}_j}{V(E_0+\omega-E_n)}, \text{ for } i,j = x,y,z. \tag{42}$$

Analysis

Equations (28) and (42) present the analytical results of the permittivity and permeability of cotinine molecule in electromagnetic field. According to the expressions of these two quantities, they can be negative simultaneously when the second parts of the expressions greater than unity. In order to fulfill this requirement, the denominators of the second part should be small enough. In other words, $E_0+\omega-E_n$ needs to be much smaller than numerator which means $\omega \approx E_n - E_0$. For a given initial energy of the electron before transition E_0, we can observe simultaneous negative permittivity and permeability of cotinine molecules in electromagnetic field when the driving frequency ω is tuned approximately equal to the transition frequency $E_n - E_0$.
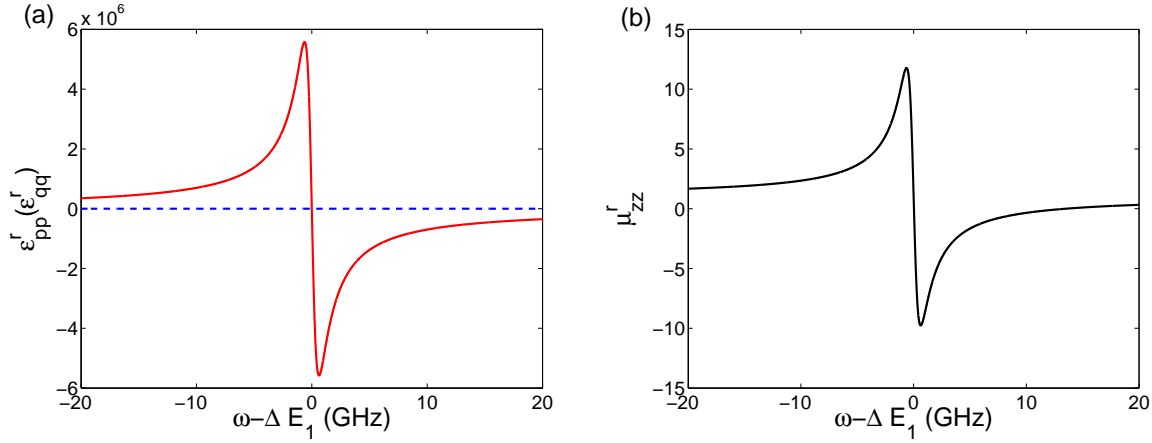
Figure 4. The numerical results of (a) permittivity and (b) permeability of cotinine molecules vs the light frequency ω. The permittivity ε_{oo}^{r} (red solid line) along one main axis in the xy plane is negative near the resonance frequency, while ε_{pp}^{r} (blue dashed line) along the other main axis is always constant. In the magnetic response, the permeability along z direction μ_{zz}^{r} is shown.

Numerical Simulation of Permittivity and Permeability

In above section, the analytical derivation suggests that permittivity and permeability of cotinine molecules might be negative simultaneously in certain frequency regime. Here we show and analyze the numerical result. In the simplified model, the cotinine molecule is simplified into a pyridine and a methyl, c.f. Figure 1 (b). The simplified cotinine model is a two dimensional model. Thus, we only need to analyze the electromagnetic responses of the molecules in x and y directions. Figure 4 shows the numerical simulation of relative dielectric constants in the xy plane and relative magnetic permittivity in z direction of the system. Here we assume the site energies $\alpha_C = 0$, $\alpha_N = 0.5\beta_{CC}$, and the coupling strengths $\beta_{CC} = -3.6$eV, $\beta_{CN} = 0.8\beta_{CC}$.[52] The excited-state life time $\tau = 10$ns is within the range of experimentally observation, e.g. 90μs.[53] For a transition to the first excited state, e.g. a spin up electron is excited from ε_3 to ε_4, the contributions from transition dipoles μ_{01} and m_{01} are much larger than others i.e., $\omega \sim \Delta E_1 = E_1 - E_0$. In Figure 4(a), both relative dielectric contants in the two main axes ε_{pp}^{r} and ε_{qq}^{r} are different from unity in the vaccum case, as the presence of nitrogen atom breaks down the reflection symmetry along the axis connecting site 3(7) and the origin. Furthermore, Figure 4 clearly shows the negative permittivity and permeability at the same time. This result suggests that cotinine molecules can be detected by negative refraction.

Discussion

In this paper we research the optical properties of drug metabolites in latent fingermarks. All of these drug metabolites have a structure in common, i.e. SRR which could realize negative refraction. And negative refraction makes the optical properties of latent fingermark quite different between drug addicts and non-drug users which can be used to distinguish them. The latent fingermarks of these two kinds of donors are observed to be inverse in light field. The method is printing the donor's fingermarks on the transparent media and observing them in the light transmission direction on the opposite side with respect to the side for the normal refraction. Because of negative refraction, the fingermarks of drug addicts are easily observable. Without loss of generality, we take cotinine as an example to calculate electromagnetic response of metabolites in latent fingermarks of smokers. According to our analytic derivation and numerical simulation, we demonstrate the presence of negative refraction in cotinine molecules. The advantage of this method is that it is physical and non-damaged. Our method is suitable for all drug metabolites which have the SRR structure. And this method can be conveniently applied to distinguish drug addicts and non-drug users too. For example, except for cotinine, benzoylecgonine and morphine can also be detected using our method.

References

1. Veselago, V. G. The electrodynamics of substances with simultaneously negative values of ε and μ. *Sov. . Phys. Uspekhi* **10**, 509, (1968).

2. Pendry, J. B. Negative refraction makes a perfect lens. *Phys. Rev. Lett.* **85**, 85, 3966, (2000).

3. Pendry, J. B., Holden, A. J., Robbins, D. J. & Stewart, W. J. Magnetism from conductors and enhanced nonlinear phenomena. *IEEE Trans. Microwave Theory Tech.* **47**, 2075, (1999).

4. Pendry, J. B., Holden, A. J., Stewart, W. J. & Youngs, I. Extremely low frequency plasmons in metallic mesostructures. *Phys. Rev. Lett.* **76**, 4773 (1996).

5. Pendry, J. B., Holden, A. J., Robbins, D. J. & Stewart, W. J. Low frequency plasmons in thin-wire structures. *J. Phys.: Condens. Matter* **10**, 4785, (1998).

6. Luo, Y. & Zhao, R. K.; Fernandez-Dominguez, A. I.; Stefan, A. M.; John, P. B. Harvesting light with transformation optics. *Sci. Chin. Inf. Sci.* **56**, 120401, (2013).

7. Fang, Y. N., Shen, Y., Ai, Q. & Sun, C. P. Negative refraction Induced by M obius topology. *Preprint arXiv*:1501.05729.

8. Pendry, J. B., Holden, A. J., Robbins, D. J. & Stewart, W. J. Magnetism from conductors and enhanced nonlinear phenomena. *IEEE Trans. Microwave Theory Tech.* **47**, 2075, (1999).

9. Cubukcu, E., Zhang, S., Park,Y.-S., Bartal, G. & Zhang, X. Split ring resonator sensors for Infrared detection of single molecular monolayers. *Appl. Phys. Lett.***95**, 043113, (2009).

10. Clark, A. W., Glidle, A., Cumming, D. R. S. & Cooper, J. M. Plasmonic split-ring resonators as dichroic nanophotonic {DNA} biosensors. *J. Am. Chem. Soc.* **131**, 17615, (2009).

11. Pryce, I. M., Kelaita, Y. A., Aydin, K., Briggs, R. M. & Atwater, H. A. Compliant metamaterials for resonantly enhanced Infrared absorption spectroscopy and refractive Index sensing. *ACS Nano* **5**, 8167, (2011).

12. Ma, C. B., Aguinaldo, R. & Liu, Z. W. Advances in the hyperlens. *Chin. Sci. Bull.* **55**, 2618, (2010).

13. Shelby, R. A., Smith, D. R. & Schultz, S. Experimental verification of a negative Index of refraction. *Science* **292**, 77, (2001).

14. Ropp, C., Cummins, Z., Probst, R., Qin, S. J., Fourkas, J. T., Shapiro, B. & Waks, E. Positioning and Immobilization of Individual quantum dots with nanoscale precision. *Nano Lett.* **10**, 4673, (2010).

15. Smith, D. R., Pendry, J. B. & Wiltshire, M. C. K. Metamaterials and negative refractive Index. *Science* **305**, 788, (2004).

16. Decker, M., Linden, S. & Wegener, M. Coupling effects in low-symmetry planar split-ring resonator arrays. *Opt. Lett.* **34**, 1579, (2009).

17. Pryce, I. M., Aydin, K., Kelaita, Y. A., Briggs, R. M. & Atwater, H. A. Highly strained compliant optical metamaterials with large frequency tunability. *Nano Lett.* **10**, 4222, (2010).

18. Chen, W. T., Wu, P. C., Chen, C. J., Hsiao, C. T., Yang, K.-Y., Sun, S., Zhou, L., Guo, G.-Y., Zheludev, N. I. & Tsai, D. P. Optical magnetic response of upright plasmonic molecules in 3D metamaterial. SPIE Newsroom **2011.**

19. Liu, N., Liu, H., Zhu, S. & Giessen, H. Stereometamaterials. *Nat. Photonics* **3**, 157, (2009).

20. Fleming, G. R. & Wolynes, P. G. Chemical dynamics in solution. *Phys. Today* **43**, 36, (1990).

21. Szabo, A. & Ostlund, N. S. *Modern quantum chemistry, Introduction to advanced electronic structure theory*; Dover: New York, 1996.

22. Greenwood, H.H. *Computing methods in quantum organic chemistry*; Wiley-Interscience: : Weinheim, Germany, 1972.

23. Pantazis, D. A. & McGrady, J. E. A Three-state model for the polymorphism in linear tricobalt compounds. *J. Am. Chem. Soc*. **128**, 4128, (2006).

24. Pyrka, G. J., El-Mekki, M. & Pinkerton, A. A. Structure of the linear trinuclear copper complex, dichlorotetrakis-(di-2-pyridylamido)tricopper. *J. Chem. Soc., Chem. Commun.* 84, (1991).

25. Peng, S. -M., Wang, C. -C., Jang, Y. -L., Chen, Y. -H., Li, F. -Y., Mou, C. -Y. & Leung, M. -K. J. One-dimensional metal string complexes. *Magn. Magn. Mater*. **209**, 80, (2000).

26. Tsai, T. -W., Huang, Q. -R., Peng, S. -M. & Jin, B. -Y. Smallest electrical wire based on extended metal-atom chains. J. *Phys. Chem. C* **114**, 3641, (2010).

27. Chae, D. -H., Berry, J. F., Jung, S., Cotton, F. A., Murillo, C. A. & Yao, Z. Vibrational excitations in single trimetal-molecule transistors. *Nano Lett*. **6**,165, (2006).

28. Chen, I. -W. P., Fu, M. -D., Tseng, W. -H., Yu, J. -Y., Wu, S.- H., Ku, C. -J., Chen, C. -H. & Peng, S. -M. Conductance and stochastic switching of ligand-supported linear chains of metal atoms. Angew. *Chem. Int. Edit*. **45**, 5814, (2006).

29. Chen, C. C., Hsiao, C. T., Sun, S., Yang, K. Y., Wu, P. C., Chen, W. T., Tang, Y. H., Chau, Y. F., Plum, E. & Guo, G. Y. Fabrication of three dimensional split ring resonators by stress-driven assembly method. *Opt. Express* **20**, 9415, (2012).

30. Ishikawa, A. & Tanaka, T. J. Two-photon fabrication of three-dimensional metallic nanostructures for plasmonic metamaterials. *Laser Micro Nanoeng.* **7**, 11, (2012).

31. Shen, Y. & Jin, B. Y. Correspondence between Gentile oscillators and N-annulenes. *J. Phys. Chem. A* **117**,12540, (2013).

32. Shen, Y., Dai, W. S. & Xie, M. Intermediate-statistics quantum bracket, coherent state, oscillator, and representation of angular momentum [SU(2)] algebra. *Phys. Rev. A* **75**, 042111, (2007).

33. Shen, Y., Ai, Q. & Long, G. L. The relation between properties of Gentile statistics and fractional statistics of anyon. *Phys A* **389**,1565, (2010).

34. Zhang, S. & Zhang, Y. Broadband unidirectional acoustic transmission based on piecewise linear acoustic metamaterials. *Chin. Sci. Bull.* **59**, 3239, (2014).

35. Cao, J. J., Shang, C., Zheng, Y. L., Feng, Y. M., Chen, X. F., Liang, X. G. & Wan, W. J. Dielectric optical-controllable magnifying lens by nonlinear negative refraction. *Sci. Rep.* **5**, 11892, (2015).

36. Philippe, F. D., Murray, T. W. & Prada, C. Focusing on plates: controlling guided waves using negative refraction. *Sci. Rep.* **5**, 11112, (2015).

37. Paniagua-Dominguez, R., Abujetas, D. R. & Sanchez-Gil, J. A.Ultra low-loss, isotropic optical negative-index metamaterial based on hybrid metal-semiconductor nanowires. *Sci. Rep.* **3**, 1507, (2013).

38. Bi, K., Guo, Y. S., Zhou, J., Dong, G. Y., Zhao, H. J., Zhao, Q., Xiao, Z. Q., Liu, X. M. & Lan, C. W. Negative and near zero refraction metamaterials based on permanent magnetic ferrites. *Sci. Rep.* **4**, 4139, (2014).

39. Pendry, J. B., Schurig, D. & Smith, D. R. Controlling electromagnetic fields. *Science* **312**, 1780, (2006).

40. Schurig, D., Mock, J. J., Justice, B. J., Cummer, S. A., Pendry, J. B., Starr, A. F. & Smith, D. R. Metamaterial electromagnetic cloak at microwave frequencies. *Science* **314**, 977, (2006).

41. Huang, Y. & Gao, L. Equivalent permittivity and permeability and multiple Fano resonances for nonlocal metallic nanowires. *J. Phys. Chem. C* **117**, 19203, (2013).

42. Droulias, S. & Yannopapas, V. Broad-band giant circular dichroism in metamaterials of twisted chains of metallic nanoparticles. *J. Phys. Chem. C* **117**, 1130, (2013).

43. Xue, H. J., Wu, R. L. & Yu. Y. Abnormal absorption and energy flow of electromagnetic wave in ultrathin metal films. *J. Phys. Chem. C* **118**, 18257, (2014).

44. Yannopapas, V. & Psarobas, I. E. Ordered arrays of metal nanostrings as broadband super absorbers. *J. Phys. Chem. C*. **116**, 15599, (2012).

45. Zhang, F., Zhao, Q., Kang, L., Gaillot, D. P., Zhao, X., Zhou, J. & Lippens, D. Microwave Conference, 2008. EuMC 2008. 38th European 2008; Vol. *1*, 801-804.

46. Kaelberer, T., Fedotov, V. A., Papasimakis, N., Tsai, D. P. & Zheludev, N. I. Toroidal dipolar response in a metamaterial. *Science* **330**, 1510, (2010).

47. Groeneveld, G., de Puit, M., Bleay, S., Bradshaw, R. & Francese, S. Detection and mapping of illicit drugs and their metabolites in fingermarks by MALDI MS and compatibility with forensic techniques. *Sci. Rep.* **5**, 11716, (2015).

48. Wei,T. T., Zhao, L. C., Jia, J. M., Xia, H. H., Du, Y., Lin,Q. T., Lin, X. D., Ye, X. J., Yan, Z. H. & Gao, H. C. Metabonomic analysis of potential biomarkers and drug targets involved in diabetic nephropathy mice. *Sci. Rep.* **5**, 11998, (2015).

49. Boddis, A. M. & Russell, D. A. Simultaneous development and detection of drug metabolites in latent fingermarks using antibody-magnetic particle conjugates. *Anal. Methods* **31**, 519, (2011).

50. Dong, W. B., Wu, R. B., Yuan, X. H., Li, C. W. & Tarn, T.-J. The Modelling of quantum control systems. *Sci. Bull.* **60**, 1493, (2015).

51. Shen, Y., Ko, H. -Y., Ai, Q., Peng, S. -M. & Jin, B. -Y. Molecular Split-ring resonators based on metal string complexes. J. *Phys. Chem. C* **118**, 3766, (2014).

52. Salem, L. *The molecular orbital theory of conjugated systems*; W. A. Benjamin: New York, 1966.

53. Tokuji, S., Shin, J.-Y., Kim, K. S., Lim, J. M., Youfu, K., Saito, S., Kim, D. & Osuka, A. Facile formation of a benzopyrane-fused [28]Hexaphyrin that exhibits distinct M obius aromaticity. *J. Am. Chem. Soc.* **131**, 7240, (2009).

Acknowledgements

Author contributions statement

Y.S. wrote the main manuscript text and did the calculations. Y.S. and Q.A. designed the project and reviewed the manuscript.